Solid-State Characterization of Novel Active Pharmaceutical Ingredients: Cocrystal of a Salbutamol Hemiadipate Salt with Adipic Acid (2:1:1) and Salbutamol Hemisuccinate Salt

KRZYSZTOF J. PALUCH,[1] LIDIA TAJBER,[1] CURTIS J. ELCOATE,[2] OWEN I. CORRIGAN,[1] SIMON E. LAWRENCE,[2] ANNE MARIE HEALY[1]

[1]School of Pharmacy and Pharmaceutical Sciences, Trinity College Dublin, College Green, Dublin 2, Ireland

[2]Department of Chemistry, Analytical and Biological Chemistry Research Facility, University College Cork, Cork, Ireland

Received 27 December 2010; revised 21 February 2011; accepted 14 March 2011

Published online 6 April 2011 in Wiley Online Library (wileyonlinelibrary.com). DOI 10.1002/jps.22569

ABSTRACT: The production of salt or cocrystalline forms is a common approach to alter the physicochemical properties of pharmaceutical compounds. The goal of this work was to evaluate the impact of anion choice (succinate, adipate, and sulfate) on the physicochemical characteristics of salbutamol forms. Novel crystals of salbutamol were produced by solvent evaporation: a cocrystal of salbutamol hemiadipate with adipic acid (salbutamol adipate, SA), salbutamol hemisuccinate tetramethanolate (SSU.MeOH), and its desolvated form (SSU). The crystalline materials obtained were characterized using thermal, X-ray, nuclear magnetic resonance, Fourier transform infrared spectroscopy, dynamic vapor sorption (DVS), and elemental analysis. The crystal forms of SA and SSU.MeOH were determined to be triclinic, ($P\bar{1}$), and monoclinic, ($P2_1/n$), respectively. DVS analysis confirmed that SSU and SA do not undergo hydration under increased relative humidity. Both thermal and elemental analyses confirmed the stoichiometry of the salt forms. The aqueous solubilities of SA and SSU were measured to be 82 ± 2 mg/mL (pH 4.5 ± 0.1) and 334 ± 13 mg/mL (pH 6.6 ± 0.1), respectively. Measured values corresponded well with the calculated pH solubility profiles. The intrinsic dissolution rate of cocrystallized SA was approximately four times lower than that of SSU, suggesting its use as an alternative to more rapidly dissolving salbutamol sulfate. © 2011 Wiley-Liss, Inc. and the American Pharmacists Association J Pharm Sci 100:3268–3283, 2011

Keywords: cocrystals; crystal structure; desolvation; dissolution rate; solubility; solvate; thermal analysis; water sorption; X-ray powder diffraction

INTRODUCTION

Salbutamol is a β2-mimetic used as a bronchodilator, which is presented as a (±) racemic mixture in pharmaceutical inhalers (propellant based and dry powder), nebules, injections, syrups, and tablets, including controlled-release forms.[1] The hemisulfate salt [commonly referred to as salbutamol sulfate (SS)] is the most common form of salbutamol used in pharmaceutical products; however, the (*R*) salbutamol hydrochloride form is also available in the market as an inhalation solution (Xopenex™, manufactured by Sepracor Inc., Marlborough, Massachusetts, USA). Although some other salbutamol salts have been reported in the literature, that is, ethanolated salbutamol adipate and salbutamol stearate,[2] to date only two crystal structures are reported in the Cambridge Structural Database (CSD): salbutamol base (SB)[3] and SS.[4] Information about the solid-state nature of other forms of salbutamol is sparse.

From a pharmaceutical point of view, different solid-state characteristics of salt forms can result in different *in vitro* solubility and dissolution properties, which, in turn, can result in an alteration of the *in vivo* activity of the active pharmaceutical ingredient (API). In particular, for pulmonary delivery, possibilities for modification of the dissolution profile of the API from a formulation point of view are limited due to restrictions in terms of excipients that are regarded as safe for pulmonary use, and may result

Additional Supporting Information may be found in the online version of this article. Supporting Information

Correspondence to: Anne Marie Healy (Telephone: +353-1-896-1444; Fax: + 353-1-896-2783; E-mail: healyam@tcd.ie)

Journal of Pharmaceutical Sciences, Vol. 100, 3268–3283 (2011)

in additional costs and regulatory obstacles associated with the development of a new drug product. This may be avoided by the direct production of alternative crystalline forms of the API with the desired solubility and dissolution profiles. The marketed solid dosage forms contain only SS, which is freely soluble in water.[5] The advantage of prolonged-release tablets containing SS was reported in clinical studies.[6] New prolonged-release oral dosage forms containing SS include hard capsules, Ventmax™ (Chiesi Ltd., Cheadle, UK), and tablet forms: Volmax CR™ (GlaxoSmithKline plc, London, UK) and Vospire ER™ (Teva Pharmaceuticals, North Wales, Pennsylvania, USA).[7] Both prolonged-release capsules and tablets containing SS have monographs in the British Pharmacopeia.[8] A transdermal delivery patch of SS was also developed.[9]

In this study, we investigated the impact of replacing the sulfate anion in the SS salt structure by an organic dicarboxylic acid: either the four-carbon chain, succinic (butanedioic) acid, or the six-carbon chain, adipic (hexanedioic) acid, on the physicochemical characteristics of the API. These two organic acids were chosen in order to investigate the impact of small changes in the chemical structure of the coformer on the physicochemical properties of the resulting salbutamol forms. A reasonable correlation between the melting points of organic coformers and the resulting salts was previously reported for diclofenac.[10] The authors also observed a trend between the salt melting point and the logarithm of the solubility. The reported melting points of adipic and succinic acids are approximately 151°C–154°C and approximately 185°C–187°C, respectively[11]; hence, it may be hypothesized that the succinate would have a lower solubility than the adipate. On the contrary, increasing the hydrophilicity of the counterion as a means of increasing the water solubility of the resultant salt has been proposed and investigated for a series of erythromycin salts.[12] The calculated log *P*s of adipic and succinic acid are 0.356 and −0.655 respectively,[13] indicating that a salt of adipic acid may be less soluble than that of succinic acid. The study performed by Li et al.[14] successfully investigated the possibility of forming ionic (salts) or neutral (cocrystals) complexes of a heterocyclic base (an ErbB2 inhibitor for the treatment of cancer) with dicarboxylic acids comprising succinate, malonate, and maleate coformers. The acids (adipic and succinic) used in the current study have similar p*K*a values. The p*K*a1 and p*K*a2 for succinic acid are 4.21 and 5.64, respectively,[11] and for adipic acid these are 4.44 and 5.44, respectively.[11] As p*K*a values of salbutamol are 9.1 and 10.4,[15] it was expected that the new forms of the API would be novel 1:1 salts of salbutamol.

Both acids are generally recognized as safe[16,17] by the US Food and Drug Administration and listed in the European Pharmacopeia.[5] Adipic acid is currently used to produce salts of piperazine (Entacyl™) and spiramycine (Rovamycine™ injectable form).[11] Succinic acid is used to form salts of benfurodil, bamethan, chloramphenicol, cibenzoline, deanol, doxylamine, ergotamine, loxepine, metoprolol, oxaflumazine, sumatriptan, and iron (FeII).[11]

MATERIALS

Salbutamol base was obtained from CHEMOS GmbH (Regenstauf, Germany). Adipic acid and succinic acid (both 99%+ grade) were obtained from Sigma–Aldrich (Dublin, Ireland). High-performance liquid chromatography (HPLC) grade methanol was obtained from Fischer Scientific (Dublin, Ireland). Deionized water was obtained from a Purite Prestige Analyst HP water purification system (Purite Ltd., Thame, UK). Potassium bromide (KBr, FTIR grade) was obtained from Sigma–Aldrich (Dublin, Ireland). Deuterated dimethyl sulphoxide (DMSO-d_6) was obtained from Apollo Scientific Limited (Stockport, UK), and paraffin wax was obtained from BDH Laboratory Supplies (Poole, UK). All other chemicals were of analytical grade and used without further purification.

METHODS

Crystallization Studies

Attempts were made to crystallize salbutamol with adipic acid and succinic acid by solvent evaporation from ethanol, methanol, and water. The tested molar ratios of salbutamol to the acid were: 1:2, 1:1, and 2:1 for each solvent, respectively. It was observed that successful crystallization was achieved only for salbutamol mixed with adipic acid in 1:1 molar ratio using methanol or water as the solvent, and for salbutamol and succinic acid mixed in 2:1 molar ratio using methanol (details of the procedure are described below). Other combinations resulted in either crystallization of one or two of the components separately or in the production of a glassy/amorphous material.

The crystals subsequently used for single-crystal X-ray and other analyses were prepared from saturated solutions, which were obtained by introducing an excess of raw material into the appropriate solvent at ambient conditions and shaking for 1 h on a WhirliMixer® (Fisons Scientific Equipment, Loughborough, UK). Ten milliliters of the suspension obtained was filtered through a 0.22-μm membrane filter into a glass vial, which was kept in a glove box (Clean Sphere CA 100, Safetech Ltd.) under constant nitrogen flow at room temperature (20°C–23°C). The moisture content in this controlled environment was less than 1% of relative humidity (RH).

Dry nitrogen flow and temperature control were provided to maintain reproducible conditions of solvent evaporation. Crystallization of salbutamol

adipate (SA) from methanol resulted each time in a very rapid nucleation of the crystals. Modification of the environmental conditions, including slowing down the evaporation rate of methanol and decreasing the temperature, did not retard the crystal growth. Very small crystals with crystal defects (inclusions) were not of sufficiently good quality to be analyzed by single-crystal X-ray analysis. A change of the solvent to water resulted in slow crystal growth and good quality crystals of SA, with a powder X-ray diffraction (PXRD) pattern consistent with that obtained for crystals produced from methanol; hence, the SA crystals obtained from water were later used for single-crystal X-ray analysis.

Preparation of Salbutamol Adipate and Succinate

A stoichiometric mixture of salbutamol and adipic acid in a 1:1 molar ratio was dissolved in methanol at 0.05 g/mL concentration of solid at 25°C. Methanol was evaporated under forced air flow at an evaporation rate of 0.4 g/min (monitored using a balance every 5 min) while stirring. The white precipitate was filtered close to the end of the methanol evaporation. The precipitate was dried for 1 h under constant air flow at 25°C. The dry powder was subjected to elemental analysis, and was determined to be salbutamol monoadipate (SA). It was obtained with a 95% yield.

A stoichiometric mixture of salbutamol and succinic acid in a 2:1 molar ratio was dissolved in methanol at 0.05 g/mL concentration of solid at 25°C. Methanol was evaporated under forced air flow at an evaporation rate of 0.4 g/min (monitored using a balance every 5 min) while stirring. After nucleation of the salt, the temperature was dropped to 20°C, and the evaporation rate of methanol was kept constant (0.4 g/min) until the concentration of the solid in methanol reached 0.1 g/mL. The white precipitate was filtered and dried at 25°C. Elemental analysis of the white crystalline powder determined it to be salbutamol hemisuccinate tetramethanolate (SSU.MeOH). It was obtained with a 80% yield. Further drying of the precipitate under constant air flow at 25°C for 24 h resulted in formation of desolvated salbutamol hemisuccinate (SSU).

Single-Crystal X-Ray Diffraction

X-ray diffraction measurements were made on a Bruker APEX II DUO diffractometer (Bruker, Billerica, Massachusetts, USA) using graphite monochromatized Mo Kα radiation ($\lambda = 0.7107$ Å), and an Oxford Cryosystems COBRA (Oxford Cryosystems Ltd., Oxford, UK) fitted with a N2 generator. All calculations were made using the APEX2 software (APEX2 v2009.3-0, Bruker AXS, 2009; SHELX)[18] and the diagrams were prepared using Mercury.[19]

CCDC 801059 (SA) and 801060 (SSU.MeOH) contain the supplementary crystallographic data for this paper. These data can be obtained free of charge from The Cambridge Crystallographic Data Center via www.ccdc.cam.ac.uk/data_request/cif.

Powder X-Ray Diffraction

Powder X-ray diffraction analysis was conducted using a Rigaku Miniflex II desktop X-ray diffractometer (Rigaku, Tokyo, Japan) fitted with an Ilaskris cooling unit operating at 30 kV and 15 mA. Ni-filtered Cu Kα radiation ($\lambda = 1.5408$ Å) was used. Room temperature measurements were recorded for the range 5°–40° 2θ at a step size of 0.05°/s.[20]

Differential Scanning Calorimetry

Differential scanning calorimetry (DSC) experiments were performed using a Mettler Toledo DSC 821^e (Mettler Toledo, Greifensee, Switzerland) with a refrigerated cooling system, LabPlant RP-100. Nitrogen was used as the purge gas. Aluminum sample holders were sealed with a lid and pierced to provide three vent holes. Sample volume was sufficient to provide proper contact between the powder and the bottom of the pan, and sample weight was at least 5 mg. DSC measurements were carried out at a heating/cooling rate of 10°C/min.[21] The DSC system was controlled by Mettler Toledo STAR^e software (version 6.10) working on a Windows NT operating system. The unit was calibrated with indium and zinc standards.

Thermogravimetric Analysis

Thermogravimetric analysis (TGA) was performed using a Mettler TG 50 module (Mettler Toledo, Greifensee, Switzerland) linked to a Mettler MT5 balance (Mettler Toledo, Greifensee, Switzerland). Samples were placed into open aluminum pans (5–12 mg). A heating rate of 10°C/min was implemented in all measurements.[21] Analysis was carried out in the furnace under nitrogen purge and monitored by Mettler Toledo STAR^e software (version 6.10) with a Windows NT operating system.

Solid-State Fourier Transform Infrared Spectroscopy

Infrared spectra were recorded on a Nicolet Magna IR 560 E.S.P. spectrophotometer equipped with MCT/A detector, working under Omnic software version 4.1. A spectral range of 650–4000 cm^{-1}, resolution 2 cm^{-1}, and accumulation of 64 scans were used in order to obtain good quality spectra. A KBr disk method was used with a 0.5%–1% sample loading. KBr disks were prepared by direct compression under 8 tonne pressure for 1 min.[22] The sample preparation did not affect the spectra, as confirmed with an attenuated total reflectance spectrometer (data not shown). The Omnic 4.1^{TM}–FTIR spectra analysis with baseline auto correction software was used to analyze the data.

Nuclear Magnetic Resonance (^{1}H NMR, ^{13}C NMR)

A Bruker Avance 400 NMR (Bruker, Billerica, Massachusetts, USA) with a four-nucleus (^{1}H, ^{13}C, ^{31}P, and ^{19}F) probe was used for NMR studies. Deuterated DMSO-d_6 was used to prepare the samples. Sample concentration was in the range 20–40 mg/mL. Spectrometer frequency was 400 MHz with an acquisition time of 2 s. The number of scans was appropriate to gain good quality spectra. Standard pulse sequence supplied by Bruker was used for ^{1}H, DEPT-90, DEPT-135, ^{13}C, and two-dimensional CH-COSY experiments. The TopSpin 2.1™ software was used to evaluate ^{1}H NMR and ^{13}C NMR results.

Elemental Analysis

Elemental analysis was carried out using an Exeter Analytical CE440 CHN analyzer (Exeter Analytical Ltd., Coventry, UK). The molar amount of carbon as carbon dioxide, nitrogen as nitrogen oxide, and hydrogen as water was determined by oxidation of the sample (around 10 mg) and thermal conductivity analysis of the gases obtained.[23]

Dynamic Vapor Sorption

Vapor sorption experiments were performed on a Dynamic Vapor Sorption (DVS) Advantage-1 automated gravimetric vapor sorption analyzer (Surface Measurement Systems Ltd., London, UK). The temperature was maintained constant at $25.0 \pm 0.1^\circ$C. Around 10 mg of powder was loaded into a sample net basket and placed in the system. The samples were equilibrated at 0% of RH until the dry, reference mass was recorded. The samples were exposed to the following percentage of RH profile: 0%–90% in 10% steps and the same for desorption. At each stage, the sample mass was equilibrated ($dm/dt \leq 0.002$ mg/min for at least 10 min) before the change of RH. An isotherm was calculated from the complete sorption and desorption profile. Amount of water was expressed as a percentage of the reference mass.

Specific Surface Area Analysis by Brunauer, Emmett, and Teller Isotherm

Samples were dried prior to analysis under nitrogen flow at 50°C for 12 h using a Gemini SmartPrep drying station (Micromeritics, Norcross, Georgia, USA). To determine the bulk specific surface area, a Micromeritics Gemini VI surface area analyzer (Micromeritics, Norcross, Georgia, USA) was used. Compressed nitrogen was used as an adsorptive gas. Each measurement consisted of six steps, determining the amount of gas adsorbed at six relative pressure points in the range of 0.05–0.3 of relative pressure P/P_0, with an equilibration time of 10 s. Free space was determined separately for each sample using helium gas. Saturation pressure P_0 was determined prior to the measurement of each sample.

Particle Size

Measurements of particle size and particle size distributions were obtained using a laser diffraction particle sizer Mastersizer 2000 (Malvern Instruments Ltd., Malvern, UK). Particles were dispersed using a Scirocco dry feeder instrument (Malvern Instruments Ltd., Malvern, UK) with 2 bar pressure. An obscuration rate of 0.5%–6% was obtained under a vibration feed rate of 50%.

Solubility Studies

Powdered SA, SSU, and SB were added in excess (approximately three times the expected saturated concentration of salbutamol) directly to 2 mL of water in an Eppendorf vial at 37°C.[24] In addition, the SA powder was suspended in an NaOH solution to investigate its solubility at a pH value other than that measured for the sample in pure water. The Eppendorfs were placed horizontally in a water bath and shaken at 100 cpm. Suspensions were filtered through a 0.22-μm membrane filter. The content of salbutamol in the saturated solutions was assayed by ultraviolet (UV) spectrophotometry at 276 nm (Shimadzu UV 1700 Pharmaspec). SB, SA, and SSU aliquots were diluted with water to obtain the appropriate concentration range. Samples were withdrawn and analyzed after 10, 11, and 12 h, and as equilibrium appeared to be reached after 10 h, the values were averaged over these three time points.

The content of adipic and succinic acids in SA and SSU aliquots was determined by HPLC. The HPLC system used was a Shimadzu HPLC Class VP series with a LC-10AT VP pump, autosampler SIL-10AD VP, and SCL-10AVP system controller. The mobile phase was filtered through a 0.45-μm membrane filter (Supor-450, Gelman, North Hempstead, New York, USA) before use. The HPLC method used for the analysis of the dicarboxylic acids was modified by Thoma and Ziegler[25] and Kordis-Krapez et al.[26] The analytical column used was a LiChrosorb RP-10 column (250 mm length, internal diameter 4 mm, and particle size 10 μm). UV detection was carried out at a wavelength of 210 nm and the injection volume was 20 μL.

Separation of adipic acid was carried out isocratically at ambient temperatures with a flow rate of 1 mL/min. The mobile phase consisted of methanol and phosphoric acid solution [(pH 2.1); 20:80 (v/v)].

Separation of succinic acid was carried out using a gradient method with a flow rate of 1 mL/min. The mobile phase consisted of two eluents: (a) phosphoric acid solution (pH 2.1) and (b) methanol and phosphoric acid solution [(pH 2.1); 20:80 (v/v)]. The following gradient was used: a linear gradient from 0% to 50% B over 7 min, and then a linear gradient from 50%

to 100% B over 1 min; this composition was maintained for 7 min. Then, again a linear gradient from 100% to 0% B over 10 min was applied, and the final mobile phase composition was continued further for 5 min. Under these conditions, the retention times of adipic acid and succinic acid were 4.3 and 6.5 min, respectively.

Intrinsic Dissolution Studies

Disks of SS, SSU, and SA were prepared by compressing 300 mg of the given material in an IR hydraulic press (PerkinElmer, UK). The 13-mm diameter disks had a 1.33 cm^2 top surface area. The bottom and side surfaces of the disks were coated with paraffin wax and mounted at the center of the bottom of a standard dissolution vessel.[27] Each dissolution experiment was performed in triplicate, as long as the dissolving disk kept a visibly constant surface area.

Intrinsic dissolution studies were performed with a type 2 dissolution test apparatus (VanKel VK7000 dissolution test station) equipped with VK650 heater/circulator.[5] The rotation speed of the paddle was set to 100 rpm. Nine hundred milliliters of deionized, degassed water was used as the dissolution medium, equilibrated at 37°C. To sample the dissolution medium, a standard dissolution vessel was equipped with a medium recirculation system. The dissolution medium was constantly circulated using a LSMatec peristaltic pump fitted with a 0.45-μm filter, through a 2 mm flow-through UV cuvette placed in a Cecil CE2020 UV-spectrophotometer set to 276 nm.[28] The rate of medium circulation was set to 25 mL/min, and the pH of the aqueous medium was monitored using a Thermo Orion 420+ pH meter.

Statistical Analysis

Statistical analysis was carried out using Minitab™ statistical software, version 14 (Minitab Inc.). Two-sample *t*-tests were carried out at a significance level of 0.05, with a *p*-value of less than 0.05 taken as significant, indicating that the observed difference between the means was statistically significant, that is, rejecting the null hypothesis.

Data Analysis

ACD/Chem Sketch™ freeware was used to calculate theoretical element contributions for elemental analysis and partial polarizability volumes.[29]

RESULTS AND DISCUSSION

Single-Crystal X-Ray Analysis

Single-crystal analysis of SA and salbutamol succinate (SSU.MeOH) was undertaken, the details of which are shown in Table 1. Crystals of SA are centrosymmetric, with both enantiomers present in the lattice. Figure 1a presents the atomic labeling in the unit cell of the adipate system, which has a 1:1 ratio of SB and adipic acid. The adipate exists in the lattice in both protonated [O(5)] and ionized [O(6), O(7)] forms, as shown by the C–O distances: 1.322(2) Å for the protonated form, and C(17)–O(6): 1.265(1) Å and C(17)–O(7): 1.261(2) Å for the ionized form. In addition, there is some disorder in the hydroxyl group on the stereogenic centre, C(8). Further views of the crystal packing are depicted in Figures 2a and 2b.

Crystals of SSU.MeOH (Fig. 1b) are also centrosymmetric and were determined to be solvated with methanol molecules (Figs. 2c and 2d). This was subsequently confirmed by DSC, TGA, elemental analysis, and ^{1}H NMR spectroscopy. The succinate was found in its ionized form, with C−O bond distances of 1.274(1) and 1.253(2) Å. The SSU.MeOH stoichiometry was 2:1:4.

Analysis of Hydrogen Bond Network

Analysis of the hydrogen bonds in SA (Table 2) reveals that the vast majority of these bonds occur between the hydroxyl groups on salbutamol and the ionized adipic carboxylate. This carboxylate is also hydrogen bonded to the secondary amine group of salbutamol. The protonated adipic acid does not play a crucial role in the creation of the hydrogen bond network, with only one hydrogen bond to a hydroxyl group of the salbutamol molecule.

Interestingly, analysis of the hydrogen bonds in methanolated salbutamol succinate (Table 3) reveals the crucial role of methanol in the formation of the

Table 1. Crystallographic Data for SA and SSU.MeOH

	SA	SSU.MeOH
Crystal system	Triclinic	Monoclinic
Space group, Z	$P\bar{1}$, 2	$P\ 2_1/n$, 4
Unit cell dimensions (°) and (Å)	$a = 9.733(3)$, $\alpha = 66.354(5)$	$a = 10.3934(5)$
	$b = 10.700(3)$, $\beta = 86.080(6)$	$b = 20.2011(10)$, $\beta = 114.5300(10)$
	$c = 10.926(3)$, $\gamma = 67.906(5)$	$c = 10.3962(5)$
Volume (Å^3)	961.2(4)	1985.76(17)
R1 [I > 2σ(I)], *w*R2 (all data)	0.038, 0.090	0.039, 0.104

SA, salbutamol adipate; SSU.MeOH, salbutamol hemisuccinate tetramethanolate.

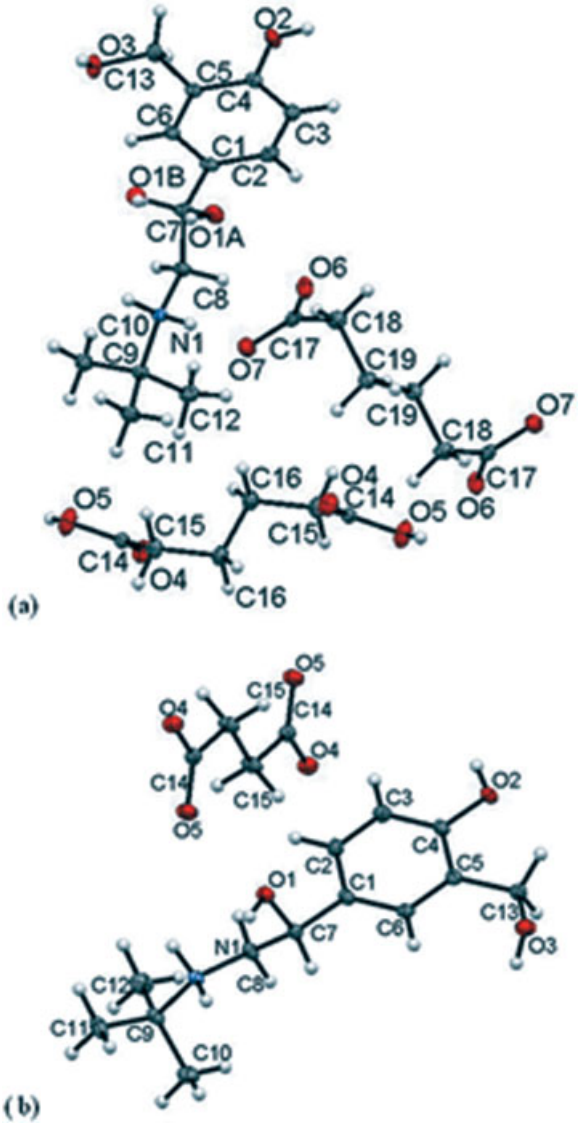

Figure 1. (a) SA and (b) SSU.MeOH showing the atomic labeling. The solvent molecules in SSU.MeOH are omitted for clarity. Probability ellipsoids are shown at the 50% level.

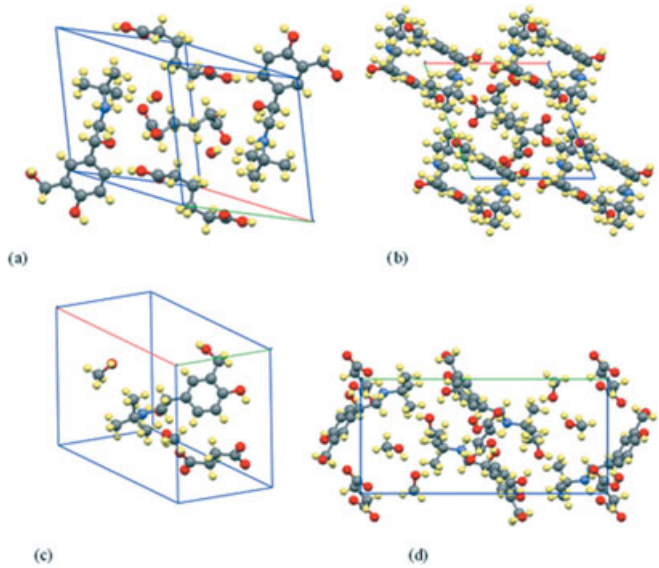

Figure 2. (a) Unit cell of SA, (b) extended packing diagram of SA along *c* axis, (c) unit cell of SSU.MeOH, and (d) extended packing diagram of SSU.MeOH along *b* axis.

lattice, and no significant interaction with the ionized succinate. Two molecules of methanol are hydrogen bonded together. There is an O−H···O interaction with the hydroxyl group of salbutamol, as well as O−H···O hydrogen bonding between the methanol hydroxyl group and salbutamol. In addition, the carboxylate of the succinate interacts with the secondary amine and a hydroxyl group of salbutamol.

A comparison of the crystal packing of SA (Figs. 2a and 2b) with SSU.MeOH (Figs. 2c and 2d) indicates why SA contains an "additional" protonated molecule of adipic acid. It can be seen that SA molecules packing along the *c* axis (Fig. 2b) consists of channels made of salbutamol molecules. These channels are placed centrally around the molecules of adipic acid. Adipic acid molecules are placed one below the other, where

Table 2. Hydrogen Bonding in SA

D−H···A	D−H (Å)	H···A (Å)	D···A (Å)	D−H···A (°)
N1−H1A···O7	0.951(19)	1.845(19)	2.7945(18)	175.6(14)
N1−H1B···O1B	0.96(2)	2.404(18)	2.808(5)	105.0(12)
N1−H1B···O6[a]	0.96(2)	1.88(2)	2.8353(18)	172.2(16)
O1A−H1C···O7[a]	0.84	1.93	2.7619(19)	169
O1B−H1D···O6[a]	0.84	2.46	2.816(5)	106
O1B−H1D···O7[a]	0.84	1.79	2.609(5)	166
O2−H2A···O6[b]	0.84	1.81	2.6327(17)	165
O3−H3A···O4[a]	0.84	1.92	2.7437(18)	167
O5−H5···O3[c]	0.88(3)	1.76(3)	2.6314(18)	172(2)
C6−H6···O3	0.95	2.50	2.8470(19)	101
C8−H8B···O2[d]	0.99	2.54	3.457(2)	154
C16−H16A···O1B[a]	0.99	2.29	3.148(5)	144

Symmetry codes: [a] 1 − x, −y, 1 − z; [b] 1 − x, −y, 2 − z; [c] 1 + x, 1 + y, −1 + z; [d] −x, −y, 2−z.
SA, salbutamol adipate.

Table 3. Hydrogen Bonding in SSU.MeOH

D—H···A	D—H (Å)	H···A (Å)	D···A (Å)	D—H···A (°)
O1—H1···O5[a]	0.84	1.79	2.6297 (14)	173
N1—H1A···O4[a]	0.929 (18)	1.852 (19)	2.7786 (15)	175.0 (13)
N1—H1B···O1[b]	0.912 (16)	1.924 (17)	2.7953(13)	159.1 (17)
O2—H2A···O7[c]	0.84	1.80	2.6312(16)	171
O3—H3A···O4[d]	0.84	1.85	2.6721(13)	165
O6—H6A···O3[e]	0.84	1.84	2.6754(13)	174
O7—H29···O6[f]	0.84	1.81	2.6523(15)	176
C2—H2···O5[g]	0.95	2.53	3.4744(14)	177
C6—H6···O3	0.95	2.56	2.8788(14)	100
C8—H8A···O2[d]	0.99	2.38	3.3068(15)	155
C11—H11B···O2[h]	0.98	2.57	3.5145(15)	162

Symmetry codes: [a] 1 + x, y, z; [b] 2 − x, 2 − y, 2 − z; [c] x, 1 + y, z; [d] 1 − x, 2 − y, 1 − z; [e] x, −1 + y, z; [f] −1/2 + x, 1/2 − y, 1/2 + z [g] 1 − x, 2 − y, 2 − z; [h] 3/2 − x, −1/2 + y, 3/2 −z.

SSU.MeOH, salbutamol hemisuccinate tetramethanolate.

ionized and protonated molecules are placed alternately in each layer. The ionized carboxylic groups of adipic acid face toward the secondary amine moieties of salbutamol molecules, whereas protonated groups are placed in close proximity to methoxyls of the benzene ring of salbutamol molecules. This indicates that the ionized acid stabilizes more polar parts of the salbutamol molecule, where partial polarizability (α) of R–NH–Me–MeOH molecule fragment was calculated to be 15.68 ± 0.5 Å^3, whereas the protonated molecule is responsible for interaction with less polar parts of salbutamol, where partial polarizability (α) of HOMe–Ar part was calculated to be 12.96 ± 0.5 Å^3. The interaction is promoted by the close proximity of carboxylic acid groups to the channels formed by salbutamol molecules. This is due to the length of adipic acid being similar to the length of the channel, with the O(5)-O(5) distance being approximately 8 Å.

Succinic acid is much shorter than adipic acid; the O(5)–O(4) distance is approximately 5 Å and forms a different arrangement to SA along the *c* axis. Despite the fact that the p*K*a(s) 1,2 of succinic acid (4.21 and 5.64 at 25°C)[11] and adipic acid (4.44 and 5.44 at 25°C)[11] are only slightly different, this difference seems to be large enough to allow ionized succinic acid to stabilize the amine group and neighboring hydroxyl of salbutamol simultaneously. In SSU.MeOH, each salbutamol molecule is stabilized, as described, by a succinic acid from one side and a second molecule of salbutamol; in that, the amine group of SB(A) interacts with the hydroxyl next to the amine group of SB(B). The solvated nature of SSU.MeOH arises from the interaction of H-bond dimers (as later described in hydrogen bond network analysis) of methanol with hydroxyls of salbutamol.

Haynes et al.[30] presented a review, reporting the occurrence of pharmaceutically acceptable anions and cations in the CSD. No examples of a cocrystal of a salt of adipic acid were reported and only 23 cocrystalline forms of adipic acid were found. The same report indicated the occurrence of only nine salts of succinic acid, indicating that both forms of salbutamol presented here are rare in terms of their solid-state structures. The SA reported in the current work should be classified as a cocrystal of the salbutamol hemiadipate salt with adipic acid, in contrast to the previously reported ethanolated salt of salbutamol hemiadipate.[2]

Previously, a cocrystal of the salt of the API with an unionized counterion was reported for the anticonvulsant drug valproic acid, wherein the API comprised cocrystalline form of sodium valproate salt with valproic acid.[31] The use of cocrystals in a similar manner to salts in order to alter the physicochemical properties of API has been comprehensively investigated,[32–38] although only one paper published so far reports on the coexistence of dianions and an unionized form of the acid in the same crystal lattice; similar to what we have determined for SA; it was a hydrated crystal of escitalopram oxalate with oxalic acid.[39]

Hirshfeld Surfaces Analysis

Hirshfeld surfaces analysis (Fig. 3) allowed visualization and comparison of reciprocal interactions among atoms in crystal lattices of SB and SS as compared with salbutamol adipate and succinate. The visualization is based on a three-dimensional surface surrounding a single molecule of salbutamol.

Noticeably, the same chemical structure of salbutamol may present different intensities of reciprocal interactions externally and internally to the Hirshfeld surface. Red places named "hot spots" indicate areas of salbutamol molecules wherein the interactions are the strongest, and the distance between attracting atoms is shorter than the attraction caused by van der Waals forces (corresponding to white color on Hirshfeld surface). In all derivatives of salbutamol, the most involved areas in the formation of hot spots include hydroxyl groups, wherein hydrogens and oxygens generate separate, independent crystallographic hot spots, and the secondary amine group. Hirshfeld surface analysis also confirmed that hydrogens of methyl groups of the butyl moiety, secondary methyl group, and hydrogens of the benzene ring are able to form weak hot spot interactions. It is evident that the molecule of salbutamol in the crystal structure of SB forms an intensive hot spot interaction close to O(1)−H(1), the same as in cocrystalline form of SA, whereas this interaction is visibly weaker for salbutamol molecules forming crystal structures of salt forms SS and SSU.MeOH. The intensity of hot spot interaction also differs in the case of the methoxyl group O(3)−H(3) attached to the benzene ring of salbutamol. Involvement in the strongest (the most intense red color) interaction was for O(3) of SB, a slightly weaker interaction was demonstrated by H(3) in

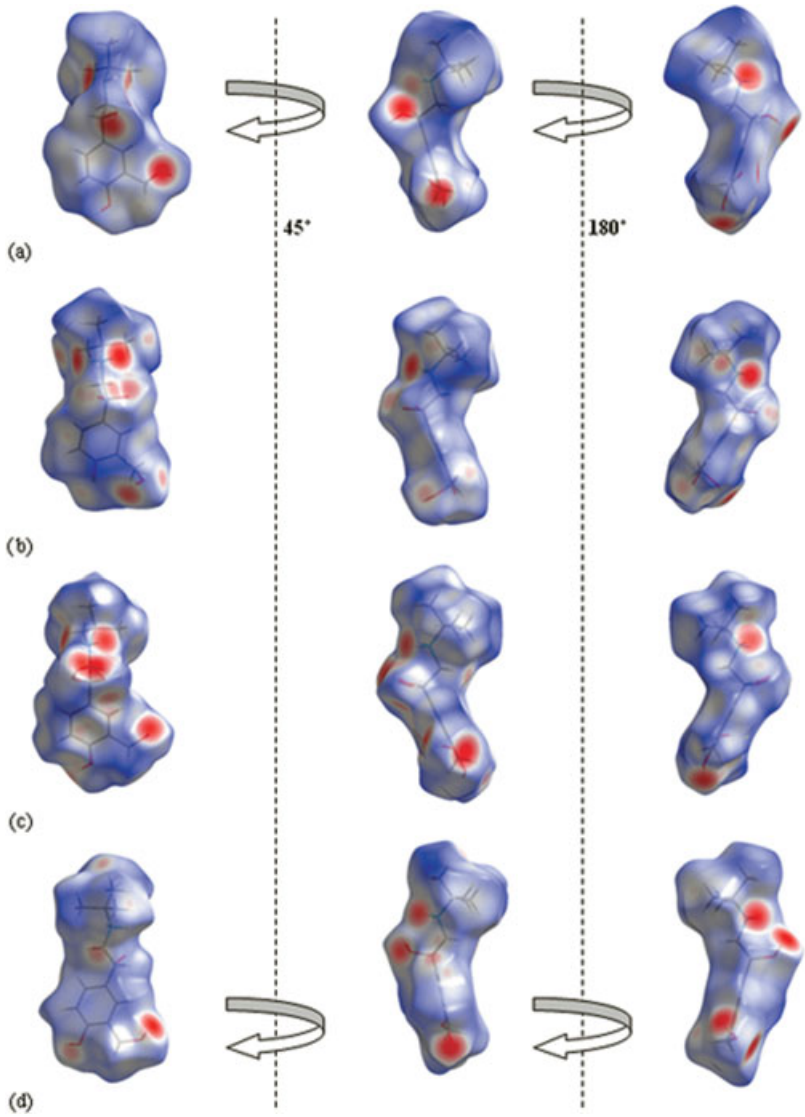

Figure 3. Hirschfield surfaces of: (a) SB, (b) SS, (c) SA, and (d) SSU.MeOH

crystal structures of SA and SSU.MeOH, whereas O(3) contact lost its intensity. The SS structure presented two weak hot spots, one from oxygen and the other from hydrogen atom. The weakest intensity and distribution on Hirshfeld surface of hot spot interactions was for SB and its cocrystalline form. The hot spot interactions identified corresponded well with the detected H-bond interactions for SA and SSU shown in Tables 3 and 4.

Results of PXRD Analysis

The theoretical powder pattern of SA generated from the single-crystal X-ray analysis at 100 K (Fig. 4a) is consistent with the PXRD pattern of the bulk material determined at ambient conditions (Fig. 4b). There are small differences between the two patterns, which most likely can be attributed to thermal anisotropic expansion of the lattice.

The bulk material consisted of colorless, transparent, rhomboidal, thin, and plate-like crystals.

Results of PXRD analysis of SSU.MeOH (Fig. 5b) are also consistent with the theoretical PXRD pattern (Fig. 5a). Again, small differences between the two patterns can be attributed to the different temperatures used for the experiments. Figure 8c presents the PXRD pattern of desolvated SSU. Broadening and lowering intensities of the Bragg peaks may be indicative of the damage to the crystal lattice.

NMR Results

Table 4 compares ^{1}H NMR data recorded for SB and the following salts: SS, SA, SSU.MeOH, and SSU. Results obtained for SB are consistent with data previously reported by Regla et al..[40] ^{1}H NMR confirmed the presence of methanol in the crystal structure due to the methyl group (3.18 ppm), which was absent in

Table 4. ^{1}H NMR Analysis of SB, SS, SA, SSU.MeOH, and SSU

	SB		SB (Regla et al.[40])	SS	SA	SSU.MeOH	SSU
Peak	ν(F1) (ppm)	Integral	ν(F1) (ppm)	ν(F1) (ppm)	ν(F1) (ppm)	ν(F1) (ppm)	ν(F1) (ppm)
C(10,11,12) H(10,11,12)	1.02	9.08	1.02	1.22	1.21	1.16	1.16
C(8)H(8/AB)	2.54	2.79	2.55	2.78	2.84	2.74	2.71
C(7)H(7)	4.40	1.09	4.42	4.69	4.70	4.61	4.59
C(13)H(13/AB)	4.48	1.99	4.47	4.50	4.48	4.59	4.49
C(2)H(2)	6.69	1.00	6.69	6.75	6.74	6.755	6.75
C(3)H(3)	6.99	1.02	6.99	7.08	7.07	7.04	7.04
C(6)H(6)	7.27	1.04	7.27	7.34	7.32	7.31	7.31
C(15,18) H(15,18/AB) C(15) H(15/AB)	–	–	–	–	2.11	2.28	2.28
C(16,19)	–	–	–	–	1.49	–	–
C(16) H(16/ABC) C(17) H(29-31)	–	–	–	–	–	3.18	–

SB, salbutamol base; SS, salbutamol sulfate; SA, salbutamol adipate; SSU.MeOH, salbutamol hemisuccinate tetramethanolate; SSU, salbutamol hemisuccinate.

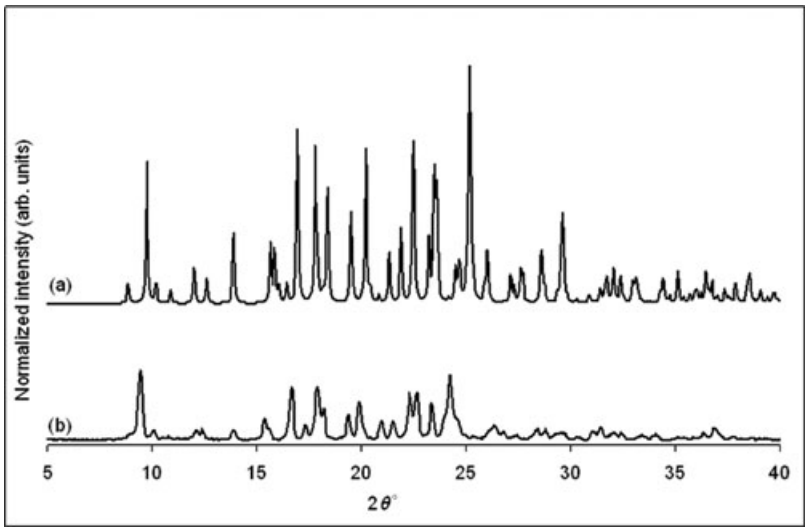

Figure 4. Comparison of SA PXRD patterns: (a) theoretical pattern and (b) experimental diffractogram.

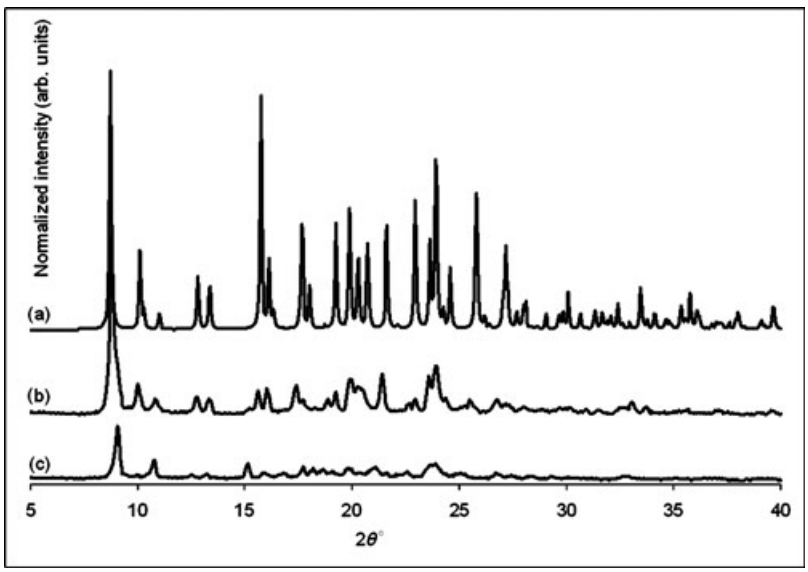

Figure 5. Comparison of PXRD patterns: (a) SSU.MeOH theoretical pattern, (b) SSU.MeOH experimental diffractogram, and (c) SSU experimental diffractogram.

Table 5. ^{13}C NMR Analysis of SB, SS, SA, SSU.MeOH, and SSU

Peak	SB ν(F1) (ppm)	SB (Regla et al.[40]) ν(F1) (ppm)	SS ν(F1) (ppm)	SA ν(F1) (ppm)	SSU.MeOH ν(F1) (ppm)	SSU ν(F1) (ppm)
C(10,11,12) H(10–12/ABC)	28.9	28.74	26.7	26.4	27.4	27.4
C(9)	49.6	49.8	49.7	49.1	50.1	50.2
C(8)H(8/AB)	50.8	50.7	49.6	49.6	49.98	50.0
C(13)H(13/AB)	58.3	58.3	58.7	58.8	58.73	58.8
C(7)H(7)	72.4	72.3	70.3	69.9	71.11	71.1
C(2)H(2)	114.0	114.0	114.6	114.7	114.60	114.6
C(3)H(3)	124.8	124.9	125.5	125.3	125.40	125.4
C(6)H(6)	125.0	125.1	125.6	125.5	125.54	125.5
C(1,4,5)	127.9	127.9	128.6	128.6	128.61	128.6
C(1,4,5)	134.6	134.5	133.4	133.3	133.79	133.8
C(1,4,5)	153.1	153.1	153.9	154.0	153.90	153.9
C(14,17)	–	–	–	176.7	176.18	176.2
C(15,18)	–	–	–	35.9	32.92	32.9
C(16,19)	–	–	–	25.6	–	–
C(17,16)	–	–	–	–	49.06	–

SB, salbutamol base; SS, salbutamol sulfate; SA, salbutamol adipate; SSU.MeOH, salbutamol hemisuccinate tetramethanolate; SSU, salbutamol hemisuccinate.

the desolvated form. Slight shifts in peak positions between SB and salbutamol salt forms may be ascribed to the interactions of molecules of dissolved APIs with DMSO.

Results of ^{13}C NMR analysis are shown in Table 5. The number and position of the carbon peaks correlate well with the data reported by Regla et al.[40] for SB. The carbons of adipic acid appeared as three peaks corresponding to six symmetrical carbons, and the carbons of succinic acid showed as two peaks corresponding to four symmetrical carbons. The ^{13}C NMR also detected the carbons (17,16) of methanol in the solvated form of SSU.MeOH, and their absence in the desolvated form SSU.

Stoichiometry and Elemental Analysis

Elemental analysis confirms the molar ratio of salbutamol and adipic acid in SA to be 1:1 (Table 6).

Elemental analysis of SSU.MeOH correlates well with the single-crystal X-ray analysis data suggesting a ratio of two molecules of salbutamol to one molecule of succinic acid to four molecules of methanol, the presence of which in the crystallized material was confirmed by NMR analysis. Results for the solvated material have greater variation due to solvate instability at ambient conditions and methanol evaporation. Results of elemental analysis confirm that the molar ratio of salbutamol to succinic acid in SSU is 2:1.

Thermal Analysis

Thermogravimetrical analysis of SA did not indicate a significant mass loss on drying at the beginning of the scan. Overall mass loss recorded during the TGA scan (Fig. 6a) up to 100°C was $0.94 \pm 0.03\%$ of the initial mass of the sample. DSC analysis of the material showed a single strong endothermal event (Fig. 6d) related to melting with decomposition at 181.00 ± 0.04°C, correlating with the beginning of significant further mass loss in the TGA. The melting point of adipic acid was measured to be 150.93 ± 0.10°C.

Differential scanning calorimetry analysis of SSU.MeOH (Fig. 6e) indicated a large broad endotherm with an onset at 69.97 ± 0.30°C and an enthalpy of 139.43 J/g. These endothermal events correlated well with the sample mass loss due to liberation of methanol (Fig. 6b) of $17.26 \pm 1.20\%$. The theoretical

Table 6. Comparison of Theoretical Values and Experimental Results of Elemental Analysis of Carbon, Nitrogen, and Hydrogen contents in Salbutamol Salts

Sample Content (%, w/w):		C %	H %	N %
SA	Theory 1:1	59.20	8.11	3.63
	Experimental	59.00 ± 0.01	8.20 ± 0.08	3.68 ± 0.07
SSU.MeOH	Theory	56.34	8.90	3.86
	Experimental	56.53 ± 0.37	8.19 ± 0.18	3.59 ± 0.53
SSU	Theory 2:1	60.38	8.11	4.69
	Experimental	60.275 ± 0.05	8.01 ± 0.07	4.61 ± 0.01

SA, salbutamol adipate; SSU.MeOH, salbutamol hemisuccinate tetramethanolate; SSU, salbutamol hemisuccinate.

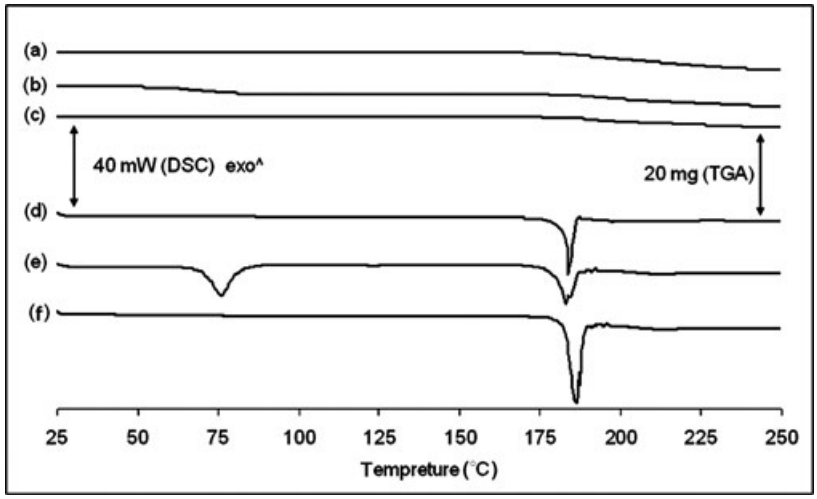

Figure 6. Thermal analysis: (a) TGA scan of SA, (b) TGA scan of SSU.MeOH, (c) TGA scan of SSU, (d) DSC of SA, (e) DSC scan of SSU.MeOH, and (f) DSC scan of SSU.

content of solvated methanol was calculated to be 17.68%.

The onset of thermal decomposition after desolvation was recorded to be at 179.23 ± 0.10°C and corresponded with further significant mass loss. In contrast, succinic acid melted at 185.90 ± 0.21°C. There was a 0.80 ± 0.02% overall mass loss up to 100°C in the TGA determined for SSU (Figs. 6c and 6f), indicating very slight drying. The onset of thermal decomposition was recorded at 182.83 ± 0.15°C.

The onsets of thermal decomposition of the new salbutamol forms were consistent with the onset of decomposition of about 180°C[41] for SS. Thus, it can be concluded that the new forms and SS have similar thermal stability.

FTIR Analysis

The FTIR patterns of SA (Fig. 7c) and SSU (Fig. 8d) differ in comparison with the spectra of the parent compounds (Figs. 7a, 7b, and 7e). The main difference between SA, SSU, and SB is the strong suppression of conjugated ≡C=C stretching vibrations of the benzene ring of salbutamol just above 1600 cm^{-1}, and changes in the intensity of the carboxylic acid ≡C=O stretch peaks. The stretching vibration of the N–H

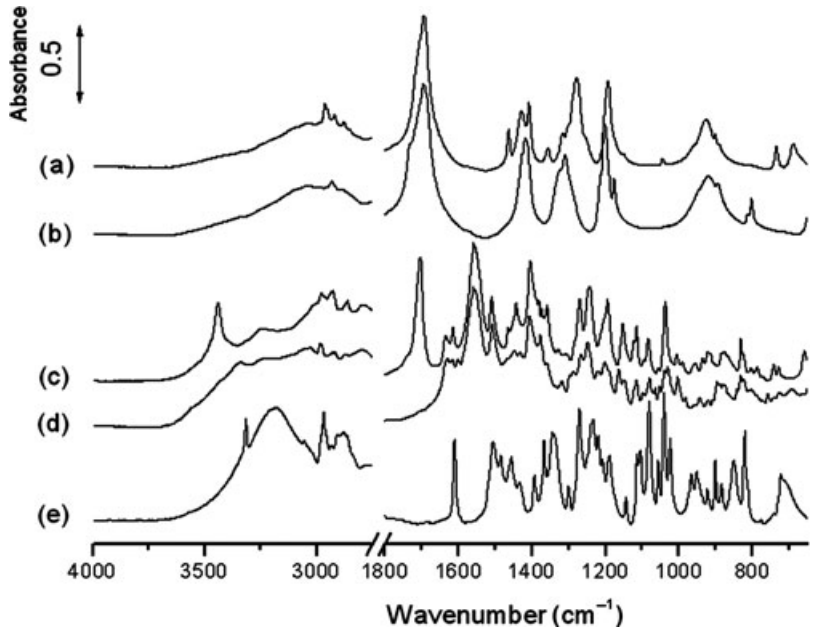

Figure 7. FTIR spectra of: (a) adipic acid, (b) succinic acid, (c) SA, (d) SSU, and (e) SB.

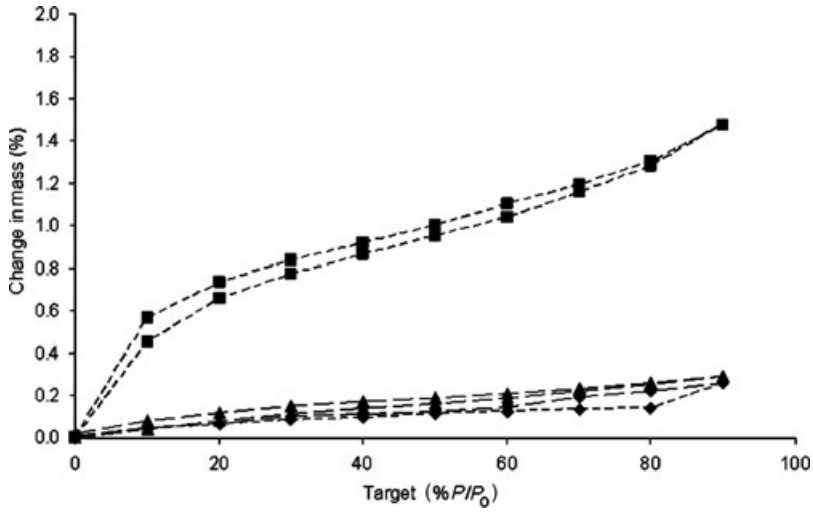

Figure 8. Dynamic vapor sorption of: (a) SA (squares), (b) SSU (triangles), and (c) SS (diamonds).

group of salbutamol (Fig. 7e) recorded at 3300 cm^{-1} for SB was nearly completely suppressed and slightly shifted toward longer wavelengths in SSU (Fig. 7d), indicating a complete ionization of the secondary amine group.In contrast, the N−H stretching vibration of the secondary amine group in SA (Fig. 7c) is relatively noticeable with a strong shift to 3450 cm^{-1}. These observations agree with the single-crystal X-ray data, suggesting a cocrystal form of SA, wherein one out of two adipic acid molecules per two molecules of SB remains unionized, but strongly H-bonded to the secondary amine group of salbutamol. The cocrystal versus salt forms of salbutamol are clearly distinguishable by FTIR, wherein the broad stretching vibration of ≡C=O of the acid in SSU has been completely suppressed, whereas the acidic carbonyl group vibration in SA remained highly visible with a slight shift toward longer wavelengths.

Dynamic Vapor Sorption

Both SSU and SA do not adsorb more than 2% of moisture, and under the conditions of DVS analysis, do not tend to form hydrates (Fig. 8). Results of equilibration of SSU at any given RH %, regardless of whether assessed in the sorption or desorption stage, are similar to SS, and in both cases, the amount of adsorbed liquid does not exceed 0.3% of the initial sample mass at 90% RH. In the case of the SA sample, less than 1.6% of the initial mass was adsorbed at 90% RH.

Because the moisture sorption behavior may be attributed to the powder surface area, the samples subjected to the DVS analysis were also characterized in terms of their specific surface area and particle size. The specific surface area (T_{BET}) of SS was measured to be $1.53 \pm 0.02\ m^2/g$, that of SA was $1.81 \pm 0.02\ m^2/g$, and T_{BET} of SSU was $2.26 \pm 0.06\ m^2/g$. The median particle size determined was 8.09 ± 0.18, 19.26 ± 0.07, and $8.73 \pm 0.09\ \mu m$ for SS, SA, and SSU, respectively. It is possible, therefore, that the higher propensity of SA to adsorb moisture may be due to the different particle size but cannot be explained by the difference in the surface area. It is likely that other surface properties, such as surface energy, contribute to this effect and will be the subject of further studies.

Solubility and Dissolution Studies

The estimated aqueous solubilities of SA, SSU, and SB were found to be 82 ± 2 mg/mL (equivalent to 0.231 ± 0.001 M of salbutamol) at pH 4.5 ± 0.1, 334 ± 13 mg/mL (equivalent to 1.183 ± 0.045 M of salbutamol) at pH 6.6 ± 0.1, and 2.63 ± 0.09 mg/mL (equivalent to 0.0110 ± 0.0004 M of salbutamol) at pH 10.0 ± 0.1, respectively. Thus the improvement in solubility, compared with SB, was 21- and 108-fold for the drug presented as SA and SSU, respectively, indicating that SSU has a fivefold greater solubility than SA.

As the new forms of salbutamol are composed of the drug and coformer that are able to ionize in solution, it is expected that the pH of the saturated medium may have a profound effect on the solubility of the compounds.[11] This was investigated for SA, as it was easier to change the pH for this compound due to the lower solubility in comparison with SSU. When the pH of medium was adjusted to 5.3, the solubility of SA was measured to be 60 ± 1 mg/mL.

Equations describing the solubility of gabapentin/3-hydroxybenzoic acid cocrystal,[42] carbamazepine, and itraconazole cocrystals have been reported.[43] These models allow relationships between the pH and cocrystal solubility to be predicted knowing only the solubility product constant (K_{sp}) and acid dissociation constants of the cocrystal constituents (pKas). Although the theoretically derived models neglect

nonidealities due to complexation and other specific interactions, very good agreements between the calculated and experimental values were observed.[42,43] This approach was employed in this work as the authors suggest that cocrystal solubility and its pH relationship may be estimated from a single measurement.[43] Similar mathematical equations were therefore developed for the new salbutamol forms to predict their solubility–pH dependence and estimate the solubility difference in relation to the pure drug. The coformers and the drug have acidic and amphoteric characteristics, respectively, therefore the previously reported equations were adapted, taking into consideration that each of the species has two pKa values and that the stoichiometry of the succinate form is 2:1.

SA has a molar ratio of 1:1, hence the equation for equilibrium reaction describing dissociation of the cocrystal in solution is as follows:

$$\mathrm{S-H_2A} \leftrightarrow S_{\mathrm{solution}} + \mathrm{H_2A_{solution}} \tag{1}$$

where S-H_2A is the cocrystal/salt in the solid phase, S_{solution} and H_2A_{solution} are equilibrium solubilities of the drug and acid, respectively, thus

$$K_{\mathrm{sp}} = \frac{[S][\mathrm{H_2A}]}{[\mathrm{S-H_2A}]}$$

and with S-H_2A in the solid phase, the K_{sp} can be presented as

$$K_{\mathrm{sp}} = [S][\mathrm{H_2A}] \Rightarrow [\mathrm{H_2A}] = \frac{K_{\mathrm{sp}}}{[S]} \tag{2}$$

Equilibrium reactions for adipic acid and salbutamol are presented in Eqs. 3 and 4 (for the acid) and Eqs. 5 and 6 (for the drug).

$$\mathrm{H_2A} \leftrightarrow \mathrm{HA^-} + H^+ \qquad K_{\mathrm{a1,H_2A}} = \frac{[H^+][\mathrm{HA^-}]}{[\mathrm{H_2A}]} \tag{3}$$

$$\mathrm{HA^-} \leftrightarrow A^{2-} + H^+ \qquad K_{\mathrm{a2,H_2A}} = \frac{[H^+][A^{2-}]}{[\mathrm{HA^-}]} \tag{4}$$

$$\mathrm{SH^+} \leftrightarrow S + H^+ \qquad K_{\mathrm{a1,S}} = \frac{[S][H^+]}{[\mathrm{SH^+}]} \tag{5}$$

$$S \leftrightarrow S^- + H^+ \qquad K_{\mathrm{a2,S}} = \frac{[S^-][H^+]}{[S]} \tag{6}$$

where $[\mathrm{HA^-}]$, $[A^{2-}]$ are concentrations of the monodissociated and fully dissociated acid species and $[\mathrm{SH^+}]$, $[S^-]$ are concentrations of protonated and monobasic salbutamol species.

Combining the total acid and drug concentrations, the solubility of SA can be expressed as (Eq. 7):

$$S_{\mathrm{cocrystal}} = \sqrt{K_{\mathrm{sp}} \times \left(1 + \frac{K_{\mathrm{a1,H_2A}}}{[H^+]} + \frac{K_{\mathrm{a2,H_2A}} \times K_{\mathrm{a1,H_2A}}}{[H^+]^2}\right)} \sqrt{\times \left(1 + \frac{[H^+]}{K_{\mathrm{a1,S}}} + \frac{K_{\mathrm{a2,S}}}{[H^+]}\right)} \tag{7}$$

where $S_{\mathrm{cocrystal}}$ is cocrystal solubility, $K_{\mathrm{a1,H2A}}$ and $K_{\mathrm{a2,H2A}}$ are the first and second dissociation constants for the acid, respectively, and $K_{\mathrm{a1,S}}$ and $K_{\mathrm{a2,S}}$ are the first and second dissociation constants for the drug, respectively.

Using a similar approach, the equation for SSU, considering the 2:1 stoichiometry, is as follows (Eq. 8):

$$S_{\mathrm{salt}} = \sqrt[3]{\frac{K_{\mathrm{sp}}}{4}\left(1 + \frac{K_{\mathrm{a1,H_2A}}}{[H^+]} + \frac{K_{\mathrm{a2,H_2A}} \times K_{\mathrm{a1,H_2A}}}{[H^+]^2}\right)} \sqrt{\times \left(1 + \frac{[H^+]}{K_{\mathrm{a1,S}}} + \frac{K_{\mathrm{a2,S}}}{[H^+]}\right)^2} \tag{8}$$

The pK_{sp} constants for salbutamol adipate and succinate, calculated using the aqueous solubility values, were 6.3 and 8.6, respectively. Substituting in pKa values as follows: $\mathrm{p}K\mathrm{a}_1 = 4.44$, $\mathrm{p}K\mathrm{a}_2 = 5.44$ for adipic acid,[11] $\mathrm{p}K\mathrm{a}_1 = 4.21$, $\mathrm{p}K\mathrm{a}_2 = 5.64$ for succinic acid,[11] and $\mathrm{p}K\mathrm{a}_1 = 9.1$, $\mathrm{p}K\mathrm{a}_2 = 10.4$ for salbutamol,[17] the pH–solubility profiles derived from Eqs. 8 and 9 are shown in Figure 9. The theoretical models suggest that a minimum SA solubility occurs at pH around 5.0 and that of SSU at pH 7.0.

The comparison of intrinsic dissolution rates (IDRs) of salbutamol from SA [4.18 mg/(cm^2 min), R^2 of 0.999] and SSU [14.94 mg/(cm^2 min), R^2 of 0.997] with that of salbutamol sulfate [15.47 mg/(cm^2 min), R^2 of 0.999] (Fig. 10) reveals that the rate of salbutamol release from SA is lower than that from SS or SSU. The IDR of salbutamol from SA is approximately four times lower and significantly different ($p < 0.05$) than that of the other salt forms, consistent with the approximately fivefold difference in salbutamol solubility. There was no significant difference ($p = 0.865$) between the IDRs of salbutamol in SS and SSU. Our results for the cocrystal of the salbutamol hemiadipate salt with adipic acid (SA) contrasts with that of Jashnani et al.[2] who obtained a salbutamol hemiadipate diethanolate, which had an IDR equivalent to SS.

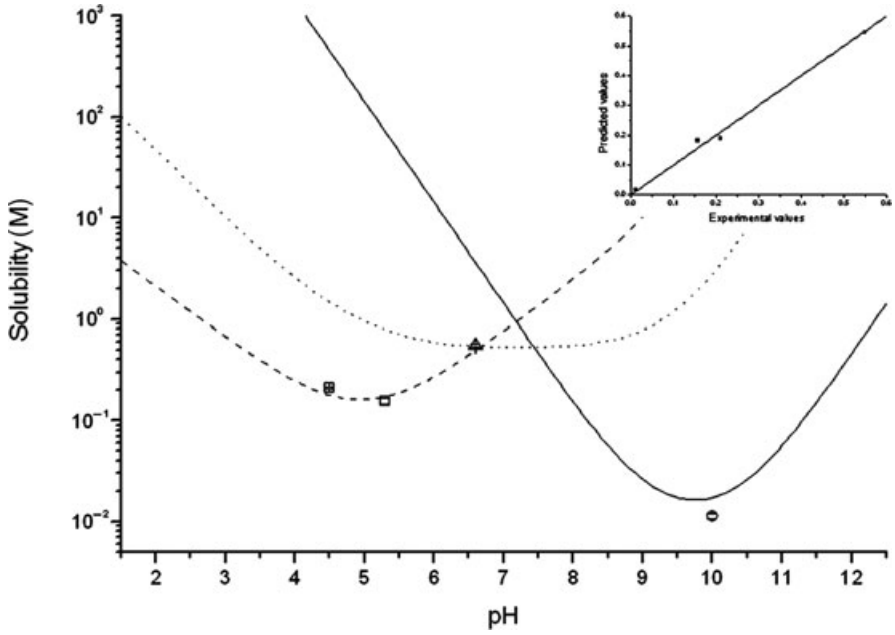

Figure 9. Theoretical profiles describing pH–solubility dependence for SA (dashed line), SSU (dotted line), and SB (solid line). Empty squares indicate experimental solubility values for SA, the triangle for SSU, and the circle shows the experimental solubility of SB. The inset shows a correlation ($y = x$) between the experimental and predicted data points.

Interestingly, the difference in the IDR values obtained reflect the different acid solubilities, that is, the saturated solubility of succinic acid at 20°C is reported to be 7.7% (w/v) and that of adipic acid to be 1.8% (w/v) [11]; therefore, it may be expected that the solubility of salbutamol adipate is lower than that of salbutamol succinate.

CONCLUSIONS

Despite the chemical similarity of succinic and adipic acid, the solid-state properties of their salbutamol salts when made by the same methods are significantly different. For the first time, we reported the involvement of adipic acid molecule in the formation of a cocrystal of a salt. Salbutamol succinate is a rare example of the succinate constituting a solvated salt form with API molecule. The IDR of salbutamol in SSU was around fourfold greater than that of SA, consistent with the approximately fivefold difference in aqueous solubility of salbutamol in SA and SSU, thus the difference in the IDRs was comparable to the solubility trend. Both materials presented similar thermal stability and did not undergo hydration under increasing humidity. The effectiveness of anion choice as a modification of *in vivo* bioavailability of

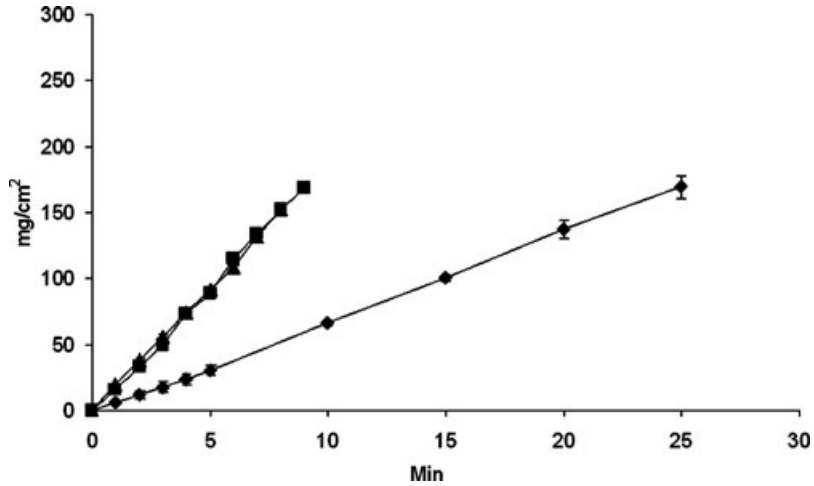

Figure 10. Intrinsic dissolution profiles of SA (diamonds), SSU (squares), and SS (triangles).

salbutamol needs further investigations, as the concept of retarding dissolution of an API by the formation of an appropriate salt/cocrystal is a promising approach, which may alleviate some issues associated with formulation of extended-release dosage forms such as component compatibility and regulatory approval for the use of excipients.

Results described here show that salt and/or cocrystal formation remains largely unpredictable and requires predominantly empirical screening. The arrangement of molecules in the crystal lattice is dependent on the geometry of the molecules involved and their potential for forming chemical interactions. Even the careful choice of similar counterions can have a profound effect on the observed crystalline lattice and further work in this area is required.

ACKNOWLEDGMENTS

The authors wish to acknowledge the funding for this research from the Irish Research Council for Science and Engineering Technology and the Solid State Pharmaceutical Cluster, supported by Science Foundation Ireland under grant number [07/SRC/B1158].

Authors would like to thank Mrs. Ann Connolly, Department of Chemistry, University College Dublin, Ireland, for elemental analysis.

REFERENCES

1. BMJ Publishing. **British National Formulary: Current edition**. Accessed October 29, 2010, at:http://bnf.org/bnf/index.htm.
2. Jashnani RN, Byron PR, Dalby RN. 1993. Preparation, characterization, and dissolution kinetics of two novel albuterol salts. J Pharm Sci 82(6):613–616.
3. Beale JP, Grainger CT. 1972. DL-N-t-Butyl-2(4-hydroxy-3-hydroxymethylphenyl)2-hydroxyethylamine, (salbutamol, Ah. 3365), C13H21NO3. Cryst Struct Commun 67(1):71–74.
4. Leger Par JM, Goursolle M, Gadret EM. 1978. Structure Crystalline du Sulfate de Salbutamol [tert-Butylamino-2 (Hydroxy-4 hydroxymethyl-3 phenyl)- 1 Ethanol. $\frac{1}{2}$ H_2SO_4]. Acta Crystallogr B34:1203–1208.
5. Council of Europe. 2007. European Pharmacopoeia. 6th ed. 5.4. Strasbourg, France: Council of Europe.
6. Vyse T, Cochrane GM. 1989. Controlled release salbutamol tablets versus sustained release theophylline tablets in the control of reversible obstructive airways disease. J Int Med Res 17(1):93–98.
7. Murthy SN, Shobharani HR. 2004. Clinical pharmacokinetic and pharmacodynamic evaluation of transdermal drug delivery systems of salbutamol sulfate. Int J Pharm 287:47–53.
8. Micromedex® Healthcare Series [intranet database]. Version 5.1. Greenwood Village, Colorado: Thomson Reuters (Healthcare) Inc.
9. British Pharmacopeia. 2010. ISBN 9780113228287. London, England: The Stationery Office.
10. O'Connor KM, Corrigan OI. 2001. Preparation and characterisation of a range of diclofenac salts. Int J Pharm 226:163–179.
11. Stahl PH, Wermuth CG. 2008. Handbook of Pharmaceutical salts properties, selection, and use. ISBN 3-906390-26-8. Weinhem, Germany, Wiley-VCH.
12. Jones PH, Rowley E, Weiss AL, Bishop DL, Chun AH. 1969. Insoluble erythromycin salts . J Pharm Sci 58 (3):337–339.
13. Veber DF, Johnson SR, Cheng HY, Smith BR, Ward KW, Kopple KD. 2002. Molecular properties that influence the oral bioavailability of drug candidates. J Med Chem 45:2615–2623.
14. Li ZJ, Abramov Y, Bordner J, Leonard J, Medek A, Trask AV. 2006. Solid-state acid-base interactions in complexes of heterocyclic bases with dicarboxylic acids: Crystallography, hydrogen bond analysis, and ^{15}N NMR spectroscopy. J Am Chem Soc 128:8199–8210.
15. Imboden R, Imanidis G. 1999. Effect of the amphoteric properties of salbutamol on its release rate through a propylene control membrane. Eur J Pharm Biopharm 47:161–167.
16. FDA. Database of Select Committee on GRAS Substances (SCOGS) Reviews, Succinic acid. Accessed December 17, 2010, at: http://www.accessdata.fda.gov/scripts/fcn/fcnDetailNavigation.cfm?rpt=scogsListing&id=339.
17. FDA. Database of Select Committee on GRAS Substances (SCOGS) Reviews, Adipic acid. Accessed December 17, 2010, at: http://www.accessdata.fda.gov/scripts/fcn/fcnDetailNavigation.cfm?rpt=scogsListing&id=9.
18. Sheldrick GM. 2008. A short history of SHELX. Acta Crystallogr A 64:112–122.
19. Macrae CF, Bruno IJ, Chisholm JA, Edgington PR, McCabe P, Pidcock E, Rodriguez-Monge L, Taylor R, van de Streek J, Wood PA. 2008. J Appl Crystallogr 41:466–470.
20. Tajber L, Corrigan DO, Corrigan OI, Healy AM. 2009. Spray drying of budesonide, formoterol fumarate, and their composites. I. Physicochemical characterisation. Int J Pharm 367:79–85.
21. Tajber L, Corrigan OI, Healy AM. 2005. Physicochemical evaluation of PVP-thiazide diuretic interactions in co-spray-dried composites—Analysis of glass transition composition relationships. Eur J Pharm Sci 24:553–563.
22. Healy AM, McDonald BF, Tajber L, Corrigan OI. 2008. Characterisation of excipient-free nanoporous microparticles (NPMPs) of bendroflumethiazide. Eur J Pharm Biopharm 69:1182–1186.
23. Paluch KJ, Tajber L, McCabe T, O'Brien JE, Corrigan OI, Healy AM. 2010. Preparation and solid state characterisation of chlorothiazide sodium intermolecular self assembly suprastructure. Eur J Pharm Sci 41:603–611.
24. Fadda HM, Sousa T, Carlsson AS, Abrahamsson B, Williams JG, Kumar D, Basit AW. 2010. Drug solubility in luminal fluids from different regions of the small and large intestine of humans. Mol Pharmacol 7(5):1527–1532.
25. Thoma K, Ziegler I. 1998. Simultaneous quantification of released succinic acid and a weakly basic drug compound in dissolution media. Eur J Pharm Biopharm 46:183–190.
26. Kordis-Krapez M, Abram V, Kac M, Ferjancic S. 2001. Determination of organic acids in white wines by RP-HPLC. Food Technol Biotechnol 39:93–99.
27. Healy AM, Corrigan OI. 1996. The influence of excipient particle size, solubility and acid strength on the dissolution of an acidic drug from two-component compacts. Int J Pharm 143(2):211–221.
28. Nocent M, Bertocchi L, Espitalier F, Baron M, Couarraze G. 2001. Definition of a solvent system for spherical crystallization of salbutamol sulfate by quasi-emulsion solvent diffusion (QESD) method. J Pharm Sci 90(10):1620–7.
29. Gad E, Mahmoud A, Khairou KS. 2008. QSPR for HLB of nonionic surfactants based on polyoxyethylene group. J Dispersion Sci Technol 29(7):940–947.
30. Haynes DA, Jones W, Motherwell WDS. 2005. Occurrence of pharmaceutically acceptable anions and cations in the Cambridge structural database. J Pharm Sci 94:2111–2120.

31. Petrusevski G, Naumov P, Jovanovski G, Bogoeva-Gaceva G, Weng Ng S. 2008. Solid-state forms of sodium valproate, active component of the anticonvulsant drug epilim. Chem Med Chem 3:1377–1386.
32. Bailey RD, Walsh MW, Bradner S, Fleischman L, Morales A, Moulton B, Rodríguez-Hornedo N, Zaworotko MJ. 2003. Crystal engineering of the composition of pharmaceutical phases. Chem Commun 2:186–187.
33. McNamara DP, Childs SL, Giordano J, Iarriccio A, Cassidy J, Shet MS, Mannion R, O'Donnell E, Park A. 2006. Use of a glutaric acid cocrystal to improve oral bioavailability of a low solubility API. Pharm Res 23(8):1888–1897.
34. Variankaval N, Wenslow R, Murry J, Hartman R, Helmy R, Kwong E, Clas SD, Dalton C, Santos I. 2006. Preparation and solid-state characterization of nonstoichiometric cocrystals of a phosphodiesterase- IV inhibitor and l-tartaric acid. Cryst Growth Des 6:690–700.
35. Zegarac M, Mestrovic E, Dumbovic A, Devcic M, Tudja P. 2007. Pharmaceutically acceptable cocrystalline forms of sildenafil. WO/2007/080362.
36. Shan N, Zaworotko MJ. 2008. The role of cocrystals in pharmaceutical Science. Drug Discovery Today 13(9–10):440–446.
37. Dova E, Mazurek JM, Anker J. 2008. Tenofovir disoproxil hemi-fumaric acid co-crystal WO/2008/143500.
38. Cheney ML, Shan N, Healey ER, Mazen H, Wojtas Ł, Zaworotko MJ, Sava V, Song S, Sanchez-Ramos JR. 2010. Effects of crystal form on solubility and pharmacokinetics: A crystal engineering case study of lamotrigine. Cryst Growth Des 10(1):394–405.
39. Harrison WTA, Yathirajan HS, Bindya S, Anilkumar HG Devaraju, 2007. Escitalopram oxalate: Co-existence of oxalate dianions and oxalic acid molecules in the same crystal. Acta Crystallogr C63:129–131.
40. Regla I, Reyes A, Körber C, Demare P, Estrada O, Juaristi E. 1997. Novel applications of raney nickel/isopropanol: Efficient system for the reduction of organic compounds. Synth Commun 27(5):817–823.
41. Larhrib H, Martin GP, Marriott C, Prime D. 2003. The influence of carrier and drug morphology on drug delivery from dry powder formulations. Int J Pharm **257**:283–296.
42. Sreenivas RL, Bethune SJ, Kampf JW, Rodriguez Hornedo N. 2009. Cocrystals and salts of gabapentin: pH dependent cocrystal stability and solubility. Cryst Growth Des 9(1):378–385.
43. Bethune SJ, Huang N, Jayasankar A, Rodriguez-Hornedo N. 2009. Understanding and predicting the effect of cocrystal components and pH on cocrystal solubility. Cryst Growth Des 9(9):3976–3988.
44. Yazan Y, Demirel M, Güler E. 1995. Preparation and *in vitro* dissolution of salbutamol sulfate microcapsules and tabletted microcapsules. J Microencapsul 12:601–607.